On Anisotropic Noise

Ares Lagae
Matthias Zwicker
Philip Dutré

Report CW 547, May 2009

Katholieke Universiteit Leuven
Department of Computer Science
Celestijnenlaan 200A – B-3001 Heverlee (Belgium)

On Anisotropic Noise

Ares Lagae
Matthias Zwicker
Philip Dutré

Report CW 547, May 2009

Department of Computer Science, K.U.Leuven

Abstract

This technical report contains errata and clarifications for the article

A. Goldberg, M. Zwicker, and F. Durand. Anisotropic noise. *ACM Transactions on Graphics*, 27(3), 2008.

Keywords : anisotropic noise.
CR Subject Classification : I.3.3, I.3.7

On Anisotropic Noise

Ares Lagae* Matthias Zwicker† Philip Dutré*
Katholieke Universiteit Leuven* University of Bern†

May 2009

This technical report contains errata and clarifications for the article
A. Goldberg, M. Zwicker, and F. Durand. Anisotropic noise. *ACM Transactions on Graphics*, 27(3), 2008.

About the Equation for the Subband Filters

Goldberg et al. provide an equation for the subband filters [Goldberg et al., 2008, equation 1], but unfortunately, the equation contains several errors. More specifically, the filters of Goldberg et al. are missing the highpass part. In this section we provide a corrected version of the equation. We reformulate the steerable filters of Portilla and Simoncelli [2000], similar as Goldberg et al., but do not square the filters.

Note that Portilla and Simoncelli and Goldberg et al. use angular frequency ω rather than frequency, for which the Nyquist critical frequency is π rather than $1/2$.

The steerable filters $D_{i,j}$ in the frequency domain are expressed in polar-separable form

$$D_{i,j}\left(r,\theta\right) = G_i\left(\theta\right) B_j\left(r\right), \tag{1}$$

where G_i is the angular part and B_j is the radial part, and i and j are indices for orientation and scale. Note that $D_{i,j}$ represents the filter, as in [Portilla and Simoncelli, 2000], and not the squared filter, as in [Goldberg et al., 2008].

The angular part G_i is

$$G_i\left(\theta\right) = \alpha_K \left|\cos^{K-1}\left(\theta - \frac{\pi i}{K}\right)\right|, \tag{2}$$

where K is the number of orientations, i is the zero-based index for orientation, and α_K is

$$\alpha_K = 2^{K-1}\frac{(K-1)!}{\sqrt{K\left(2\left(K-1\right)\right)!}}. \tag{3}$$

Note that G is squared in [Goldberg et al., 2008], and that the definition of α_K contains an error in both [Portilla and Simoncelli, 2000] and [Goldberg et al., 2008].

*e-mail: {ares.lagae,philip.dutre}@cs.kuleuven.be
†e-mail: zwicker@iam.unibe.ch

The radial part B_j is a bandpass filter obtained by multiplying a lowpass filter L and a highpass filter H. The lowpass filter L is

$$L(r) = \begin{cases} 1 & \text{if } r \leq \frac{\pi}{2}, \\ \cos\left(\frac{\pi}{2}\log_2\frac{2r}{\pi}\right) & \text{if } \frac{\pi}{2} < r < \pi, \\ 0 & \text{if } \pi \leq r. \end{cases} \tag{4}$$

Note that L corresponds to L_0 in [Portilla and Simoncelli, 2000]. The highpass filter H is

$$H(r) = \begin{cases} 0 & \text{if } r \leq \frac{\pi}{4}, \\ \cos\left(\frac{\pi}{2}\log_2\frac{2r}{\pi}\right) & \text{if } \frac{\pi}{4} < r < \frac{\pi}{2}, \\ 1 & \text{if } \frac{\pi}{2} \leq r. \end{cases} \tag{5}$$

Note that the highpass filter is missing in [Goldberg et al., 2008]. The radial part of the filter B_j is

$$B_j(r) = L\left(2^j r\right) H\left(2^j r\right), \tag{6}$$

where j is the zero-based index for scale. Note that B represents the product of the highpass filter and the angular part in [Portilla and Simoncelli, 2000], and not a bandpass filter.

The angular and radial part of the steerable filters are illustrated in figure 1.

The steerable filters $D_{i,j}$ do not sum to one, but their squares $D_{i,j}^2$ do. This is illustrated in figure 2.

A full frequency domain decomposition consists of the subband filters $D_{i,j}$, for a specific number of orientations K and scales N, complemented with a radially symmetric lowpass filter L_N and highpass filter H_N, that account for the frequencies not fully accounted for by the subband filters (e.g. $\omega < \pi/16$ and $\omega > \pi/2$ in figure 2(c)).

Figure 3, figure 4 and figure 5 illustrate the steerable filters squared.

About the Spectral Noise Synthesis

In this section we clarify the spectral noise synthesis of Goldberg et al. [2008]. It might not be immediately clear why the multiplication in the frequency domain should be performed with the square of the filters, and what the relation is between the filters and the frequency spectra.

Goldberg et al. construct the subband noise images $n_{i,j}$ using frequency filtering of white noise using the subband filters $D_{i,j}^2$

$$n_{i,j} = \mathcal{F}^{-1}\left\{D_{i,j}^2 * F\right\}, \tag{7}$$

where $\mathcal{F}$ is the Fourier transform, $*$ denotes component-wise multiplication, and $F = \mathcal{F}\{f\}$, where f is white noise. The sum of all oriented subband noise images of a specific scale results in perfectly isotropic noise of that scale, and, similarly, the sum of all subband noise images results in f

$$\sum_{i=0}^{K-1}\sum_{j=0}^{N-1} n_{i,j} = f. \tag{8}$$

These equations imply that the filters used for frequency filtering, in this case $D_{i,j}^2$, sum to one. Because the steerable filters $D_{i,j}$ do not sum to one, but their squares do, the multiplication in the frequency domain is performed with the square of the steerable filters. Note that if the filters used for frequency filtering would not sum to one, the sum of all oriented subband noise images of a specific scale would not results in perfectly isotropic noise.

Goldberg et al. start the spectral noise synthesis in the frequency domain, by creating a frequency spectrum F consisting of complex valued white noise. This is a shortcut for starting the spectral noise synthesis in the spatial domain, by creating a real valued white noise f, and computing F, by performing a Fourier transform. In this case, the band-limited spatial domain noise images $n_{i,j}$ are obtained as the real part of the inverse Fourier transform of the noise subbands $N_{i,j}$. Note that all spatial domain noise images $n_{i,j}$ must be computed from the same white noise.

The amplitude spectrum of a noise subband is given by the filter used for frequency filtering, in this case $D_{i,j}^2$. This follows from the spectral noise synthesis. Therefore, the power spectrum of the noise subband is given by $D_{i,j}^4$.

Figure 6 shows anisotropic noise synthesized using frequency filtering. Figure 7 shows the corresponding amplitude spectra. Note the similarity between the amplitude spectra and the filters squared shown in figure 5. Figure 8 shows isotropic noise obtained by summing anisotropic noise. Figure 9 shows the corresponding amplitude spectra. Note the similarity between the amplitude spectra and the radial part of the filters squared shown in figure 4. The amplitude spectra were computed using Bartlett's method of averaging periodograms [Lagae et al., 2009].

About the Steerability of the Noise

Goldberg et al. state that that the steerability property of the filters of Portilla and Simoncelli [2000] is useful because it avoids interpolation artifacts when linearly blending the subbands [Goldberg et al., 2008, section 2]. This seems to suggest that interpolating between two oriented noise subbands will result in a noise with an intermediate orientation. However, it is not clear if this is also the case. More specifically, it is not clear whether squaring the filters of Portilla and Simoncelli keeps the steerability property, and whether the least squares and heuristic approximation compute the appropriate steering weights.

About the Intensity Distribution of the Noise

Goldberg et al. use uniform white noise for spectral noise synthesis [Goldberg et al., 2008, section 2]. This might not seem appropriate since noise is usually expected to have a Gaussian intensity distribution. Although all noise subbands seem to have a Gaussian intensity distribution, even when the spectral noise synthesis is started in the spatial domain using a real valued uniform white noise, we recommend to start the spectral noise synthesis in the spatial domain using a real valued Gaussian white noise. This ensures that the full domain composition will result in Gaussian white noise.

Figure 10 shows the Gaussian intensity distribution of anisotropic noise synthesized using frequency filtering starting from real valued Gaussian white noise in the spatial domain.

About the Term Frequency Spectrum

Goldberg et al. [2008] use the term *frequency spectrum* throughout the article rather than the term *amplitude spectrum* or *power spectrum*. It might not be immediately clear that *frequency spectrum* is used in the sense of *amplitude spectrum* and not of *power spectrum*.

Acknowledgments

Ares Lagae is a Postdoctoral Fellow of the Research Foundation - Flanders (FWO), and acknowledges K.U.Leuven CREA funding (CREA/08/017).

References

A. Goldberg, M. Zwicker, and F. Durand. Anisotropic noise. *ACM Transactions on Graphics*, 27(3), 2008.

Ares Lagae, Sylvain Lefebvre, George Drettakis, and Philip Dutré. Procedural noise using sparse Gabor convolution - auxiliary material. Report CW 545, Department of Computer Science, K.U.Leuven, 2009.

Javier Portilla and Eero P. Simoncelli. A parametric texture model based on joint statistics of complex wavelet coefficients. *International Journal of Computer Vision*, 40(1):49–70, 2000.

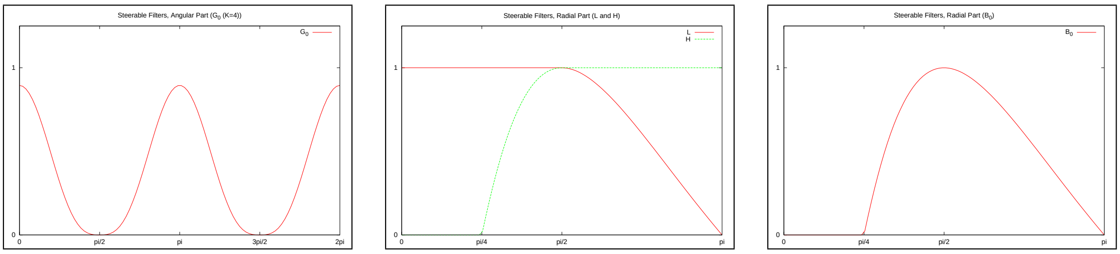

(a) Angular part (G_0). (b) Radial part (L and H). (c) Radial part (B_0).

Figure 1: Graphs of the steerable filters. (a) Angular part (G_0 ($K = 4$)). (b) Radial part (L and H). (c) Radial part (B_0).

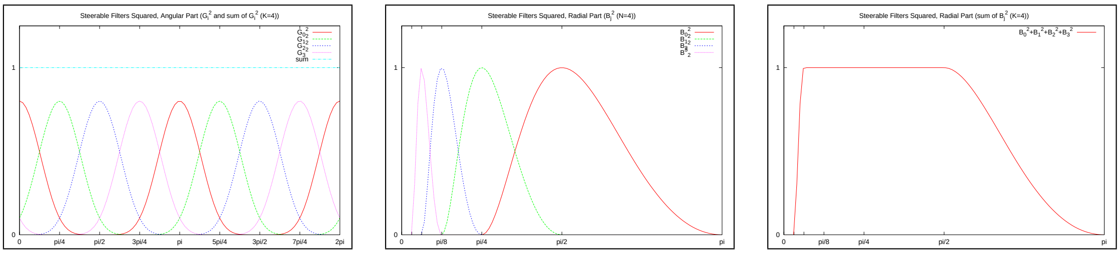

(a) Angular part (G_i^2 and $\sum G_i^2$). (b) Radial part (B_j^2). (c) Radial part ($\sum B_j^2$).

Figure 2: Graphs of the steerable filters squared. (a) Angular part (G_i^2 and $\sum G_i^2$ ($K = 4$)). (b) Radial part (B_j^2 ($N = 4$)). (c) Radial part ($\sum B_j^2$ ($K = 4$)).

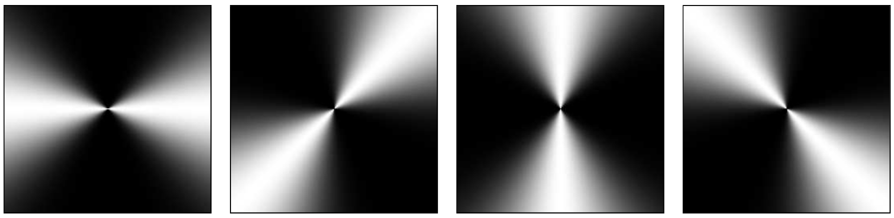

$i = 0$ $i = 1$ $i = 2$ $i = 3$

Figure 3: Images of the angular part of the steerable filters squared ($K = 4$).

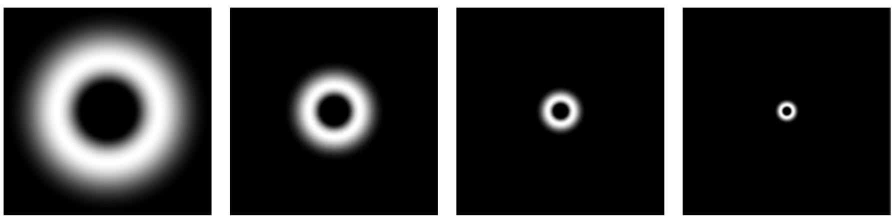

$j = 0$ $j = 1$ $j = 2$ $j = 3$

Figure 4: Images of the radial part of the steerable filters squared ($N = 4$).

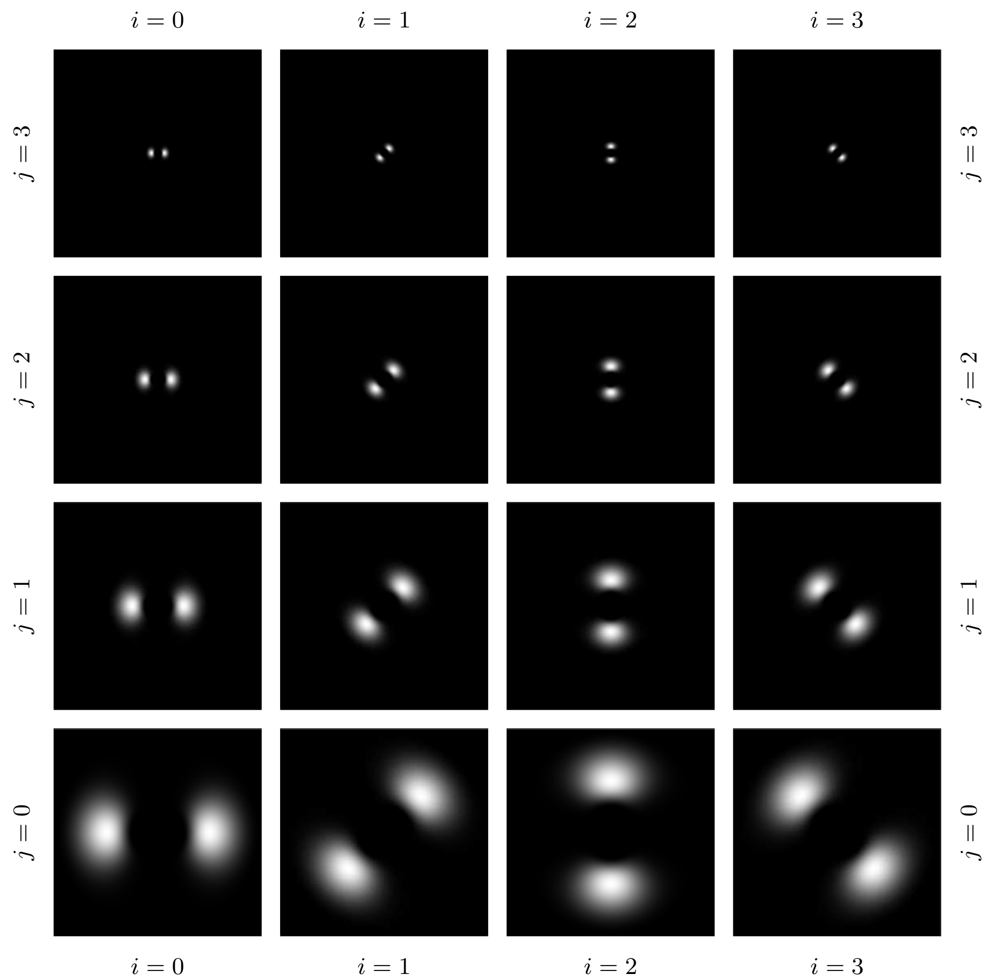

Figure 5: Images of the steerable filters squared ($K = 4$, $N = 4$).

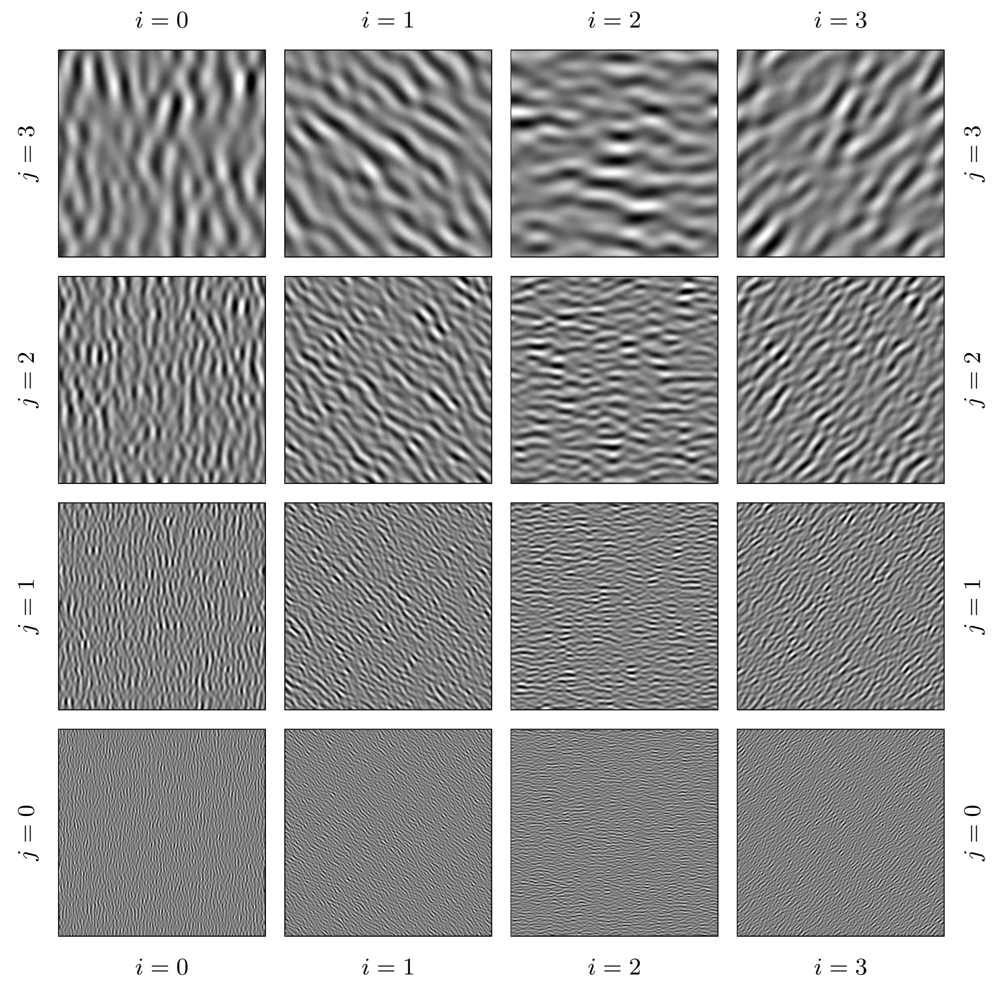

Figure 6: Anisotropic noise ($K = 4$, $N = 4$).

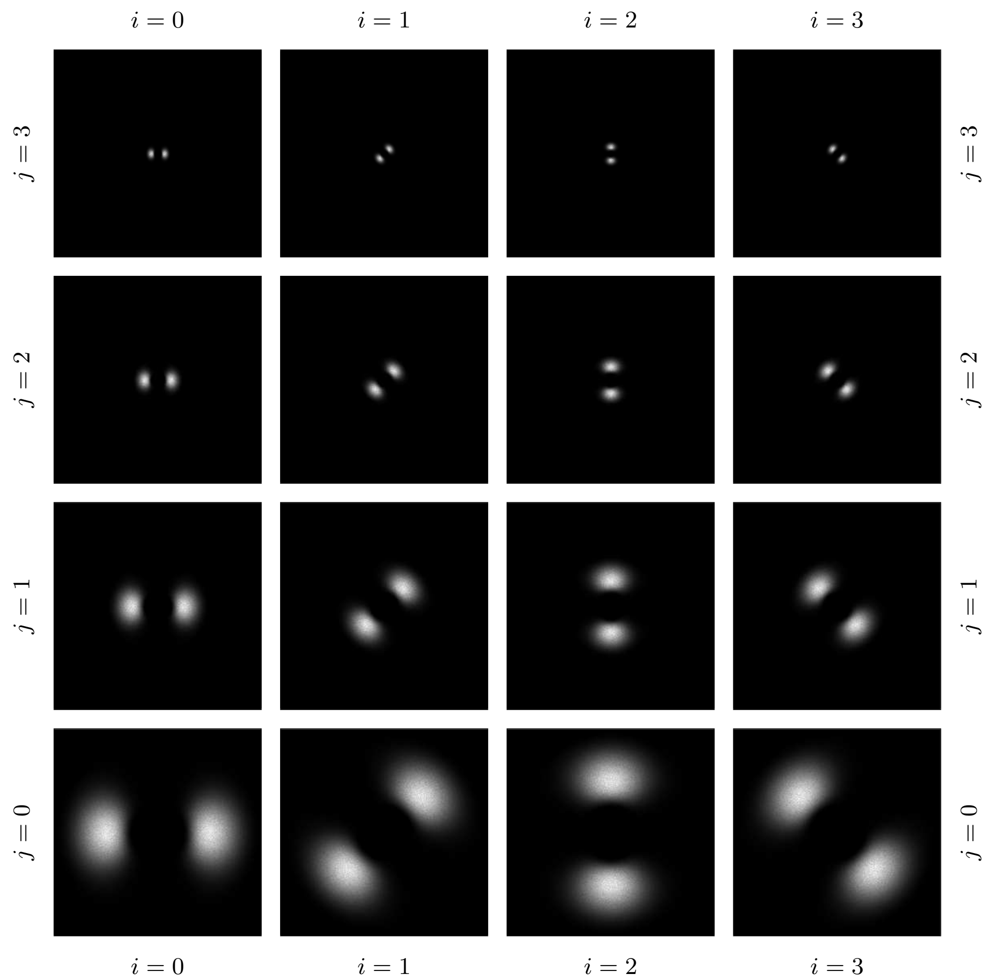

Figure 7: Amplitude spectrum of anisotropic noise ($K = 4$, $N = 4$).

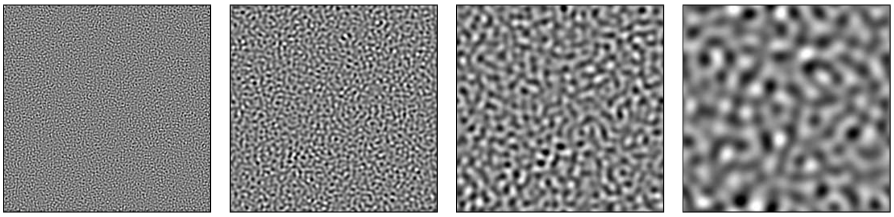

$j = 0$ $j = 1$ $j = 2$ $j = 3$

Figure 8: Isotropic noise ($N = 4$).

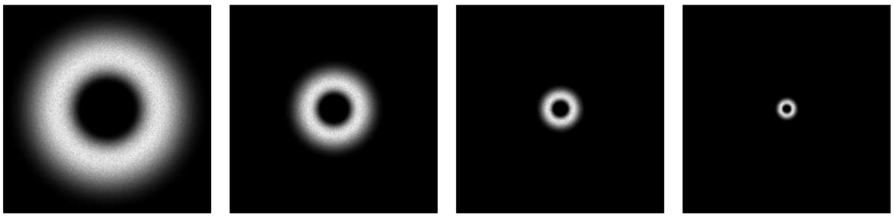

$j = 0$ $j = 1$ $j = 2$ $j = 3$

Figure 9: Amplitude spectrum of anisotropic noise ($N = 4$).

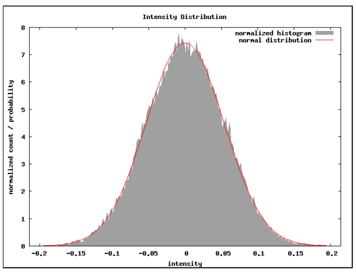

Figure 10: Intensity distribution of anisotropic noise.